Ecotoxicology and Environmental Safety 230 (2022) 113108

Contents lists available at ScienceDirect

Ecotoxicology and Environmental Safety

journal homepage: www.elsevier.com/locate/ecoenv

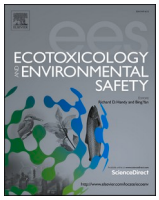

Weakened interaction of ATG14 and the SNARE complex blocks autophagosome-lysosome fusion contributes to fluoride-induced developmental neurotoxicity

Yuanli Zhang [a,b,c], Xie Han [a,b,c], Yanling Tang [a,b,c], Jingjing Zhang [a,b,c], Zeyu Hu [a,b,c], Wanjing Xu [a,b,c], Ping Yao [a,b,c], Qiang Niu [a,b,c,*]

[a] Department of Preventive Medicine, School of Medicine, Shihezi University, Shihezi, Xinjiang, People's Republic of China
[b] Key Laboratory of Preventive Medicine, Shihezi University, Shihezi, Xinjiang, People's Republic of China
[c] Key Laboratory of Xinjiang Endemic and Ethnic Diseases (Ministry of Education), School of Medicine, Shihezi University, Shihezi, Xinjiang, People's Republic of China

ARTICLE INFO

Edited by Dr. Caterina Faggio

Keywords:
Fluoride
Developmental neurotoxicity
Autophagosome-lysosome fusion
SNAREs
ATG14

ABSTRACT

Fluoride is capable of inducing developmental neurotoxicity, but the mechanisms involved remain unclear. We aimed to explore the role of autophagosome-lysosome fusion in developmental fluoride neurotoxicity, particularly focusing on the interaction between ATG14 and the soluble N-ethylmaleimide-sensitive factor attachment protein receptor (SNARE) complex. We developed in vivo models of Sprague–Dawley rats exposed to sodium fluoride (NaF) from the pregnancy of parental rats until the offspring were two months old and in vitro models of NaF and/or Ad-ATG14-treated SH-SY5Y cells. We assessed neurobehavioral changes in offspring and further investigated the effects of NaF exposure on autophagic flux, apoptosis, autophagosome-lysosome fusion, and the interaction between ATG14 and the SNARE complex. NaF exposure impaired offspring learning and memory capabilities and induced the accumulation of autophagosomes and autophagic flux blockage and apoptosis, as indicated by increased LC3-II, p62, and cleaved-caspase-3 expression in vivo and in vitro. In addition, NaF treatment downregulated the protein expression of ATG14 and the SNARE complex and induced autophagosome-lysosome fusion blockage as evidenced by decreased ATG14, STX17, SNAP29, and VAMP8 expression and diminished colocalization of autophagosomes and lysosomes in vivo and in vitro. Furthermore, ATG14 upregulation enhanced the interaction of ATG14 and the SNARE complex to facilitate autophagosome-lysosome fusion, thereby restoring autophagic flux and alleviating NaF-induced apoptosis. In conclusion, NaF exhibited developmental neurotoxicity by restraining the interaction of ATG14 with the SNARE complex and hindering autophagosome-lysosome fusion, thereby participating in the occurrence and development of fluoride neurotoxicity. Notably, ATG14 upregulation protects against developmental fluoride neurotoxicity, and ATG14 may serve as a promising biomarker for further epidemiological investigation.

1. Introduction

Fluoride is extensively but unevenly distributed in the natural environment. Sources of fluoride intake include foods, water and air, pesticide residues, supplements, industrial emissions, and certain pharmaceuticals (Khattak et al., 2022; Melila et al., 2022). The ingestion of appropriate amounts of fluoride is beneficial, but long-term exposure to excessive environmental fluoride results in not only dental fluorosis and skeletal fluorosis but also impairment in the nervous system. Previous literatures have demonstrated that fluoride can cross the placental barrier and blood-brain barrier during the perinatal period, accumulating in the infant's brain, which has higher affinity and absorptive proportions of fluoride than the adult brain (Hu and Wu, 1988; O'Mullane et al., 2016). Epidemiological studies, including

Abbreviations: Ad-ATG14, ATG14 overexpression; ACTB, actin beta; GAPDH, glyceraldehyde-3-phosphate dehydrogenase; PND, postnatal day; RAPA, rapamycin; SNAP29, synaptosome-associated protein 29; SNARE, soluble N-ethyl amide-sensitive factor attachment protein receptor; STX17, syntaxin 17; VAMP8, vesicle-associated membrane protein 8.

* Correspondence to: Department of Preventive Medicine, School of Medicine, Shihezi University, North 2nd Road, Shihezi, Xinjiang 832000, People's Republic of China.

E-mail address: niuqiang@shzu.edu.cn (Q. Niu).

https://doi.org/10.1016/j.ecoenv.2021.113108
Received 2 October 2021; Received in revised form 16 December 2021; Accepted 18 December 2021
Available online 22 December 2021

cross-sectional studies and prospective studies, have demonstrated that excessive fluoride exposure is associated with poorer IQ levels in children (Cui et al., 2018; Green et al., 2019). Animal studies have confirmed that fluoride-exposed rats during embryonic and lactation periods have poorer learning and memory abilities (Zhao et al., 2019). These results suggest that high fluoride can cause histopathological abnormalities, inflammation, and DNA damage (Bartos et al., 2018). Currently, convincing evidences suggest that the mechanisms by which fluoride affects neuronal functions include the release of cytochrome c from mitochondria, promotion of oxidative stress products (hydrogen peroxide, myeloperoxidase, and nitric oxide), and alteration of the release of the neurotransmitter acetylcholine, resulting in cell apoptosis (Tu et al., 2018; Caglayan et al., 2021). Nevertheless, more research is needed to reveal the mechanisms underlying fluoride-induced developmental neurotoxicity.

Since neurons are nonregenerative cells, they cannot remove misfolded proteins and damaged organelles by cell division. Therefore, it is essential to maintain homeostasis by removing harmful substances in neurons through autophagy. Autophagy is a dynamic self-digestion process consisting of structured and dynamically sequential stages, including initiation, extension, maturation, fusion and degradation, defined as autophagic flux. Autophagic flux blockage is one of the potential pathogenic mechanisms contributing to developmental neurotoxicity (Wong and Cuervo, 2010). Recent studies have shown that excessive fluoride exposure impairs autophagic flux in the hippocampus, leading to cell apoptosis (Zhou et al., 2019). Moreover, autophagic flux blockage can cause the accumulation of damaged organelles and other useless cell components, resulting in cell death (Li et al., 2019). Intriguingly, the autophagy agonist rapamycin protects SH-SY5Y cells from defective autophagy and excessive apoptosis by targeting the inhibition of mTOR, thereby enhancing neuronal survival (Zhou et al., 2019). Although some literatures have revealed potential associations between autophagic flux blockage and fluoride-induced developmental neurotoxicity, the precise mechanisms underlying this process remain unclear.

Autophagosome-lysosome fusion is a prerequisite of autophagic flux and is crucial for normal autophagic function (Li et al., 2019). The fusion is regulated by multiple factors and involves many genes and signaling pathways. Soluble N-ethylmaleimide-sensitive factor attachment protein receptor (SNARE) complex, including STX17, SNAP29, and VAMP8 (Itakura and Mizushima, 2013), plays an integral role in this fusion process. STX17, recruited by mature autophagosomes, combines with SNAP29 to form a primary complex via a closely packed hairpin-type structure. Next, SNAP29 binds with lysosome-localized VAMP8 using covalent bonds to form the STX17-SNAP29-VAMP8 complex, mediating the membrane fusion process between autophagosomes and lysosomes (Bernard and Klionsky, 2015). The STX17-SNAP29-VAMP8 complex is the core factor involved in autophagosome-lysosome fusion, and recent studies have found that ATG14 is a requisite switch that controls the formation of the SNARE complex (Diao et al., 2015). ATG14 is located upstream of autophagy and is essential in regulating autophagosome-lysosome fusion (Diao et al., 2015). Through the coiled-coil structural domain of ATG14, it binds to the SNARE core domains of STX17 and SNAP29, enhancing the stability of the STX17-SNAP29-VAMP8 complex and promoting autophagosome-lysosome fusion (Liu et al., 2015). Mounting evidence suggests that autophagosome-lysosome fusion blockage has been implicated as an important cause of several diseases, including neurodegenerative diseases and developmental neurotoxicity (Ji et al., 2021; Ji and Zhao, 2021). Previous studies revealed that fluoride can block autophagic flux, leading to autophagic degradation disorder and neurological damage (Niu et al., 2018), and the specific reason remains largely unknown. Given that impaired autophagosome-lysosome fusion is an important cause of autophagic flux blockage and impaired autophagic degradation, in-depth studies regarding whether NaF disrupts autophagoso me-lysosome fusion in the nervous system and whether this disruption leads to weakened interaction between ATG14 and the SNARE complex are still lacking.

Therefore, we utilized an in vivo SD rat model of ingesting fluoridated water ad libitum from the pregnancy of parental rats until two months old of offspring (simulating human exposure and covering critical periods of neurological development) and an in vitro model of NaF-treated SH-SY5Y cells, which is generally used to study developmental neurotoxicity (Qiao et al., 2005; Zhao et al., 2019; Martínez et al., 2020), as well as the molecular intervention of ATG14 in NaF-treated SH-SY5Y cells, to explore the role and mechanism of autophagosome-lysosome fusion on neuronal development following NaF exposure, particularly focusing on the interaction of ATG14 and the SNARE complex.

2. Materials and method

2.1. Chemicals and reagents

The following antibodies were used: anti-LC3 (18725–1-AP, Proteintech, USA), anti-p62 (18420–1-AP, Proteintech, USA), anti-cleaved-caspase-3 (19677–1-AP, Proteintech, USA), anti-PARP1 (13371–1-AP, Proteintech, USA), anti-ATG14 (28021–1-AP, Proteintech, USA), anti-STX17 (17815–1-AP, Proteintech, USA), anti-SNAP29 (12704–1-AP, Proteintech, USA), anti-VAMP8 (15546–1-AP, Proteintech, USA), anti-GAPDH (60004–1-Ig, Proteintech, USA), and anti-β-actin (BM0627, Boster, China). The following chemical reagents were used: NaF, (Sigma–Aldrich CO., St Louis, MO, USA), rapamycin (RAPA, S1039, Selleck, USA), Dulbecco's modified Eagle's medium (DMEM, 11965–092, Gibco, USA), Annexin V-FITC/PI apoptosis detection kit (70-AP101–100, MultiSciences, China), and Cell Counting kit-8 (CCK-8, CK04, Dojindo, Japan). A recombinant adenovirus with ATG14 overexpression was also developed (PHBAP-ATG-071, Hanbio Biotechnology, China). All of the other reagents were analytical grade and purchased locally.

2.2. Animals and treatments

The Experimental Animal Center of Xinjiang Medical University provided adult Sprague–Dawley (SD) rats, license number: SCXK (Xinjiang) 2018–0003. The rats were kept at a constant humidity (50%–60%) and temperature (20–25 ℃). All animal experiments related to this study were authorized by the Animal Research Ethics Committee of the School of Medicine, Shihezi University, and all operations were strictly implemented under relevant guidelines. Research ethics approval has been provided in the Supplementary material. All rats were maintained using tap water and standardized granular food in plastic cages.

After seven days of acclimatization, forty-eight SD rats were randomly assigned to the control and experimental groups as follows: one control group (tap water containing less than 1 mg/L fluorine) and three NaF-treated groups (NaF was mixed in drinking water at concentrations of 25, 50, or 100 mg/L and given ad libitum, corresponding to 9.04, 22.6, or 45.2 mg/L fluorine, respectively) to imitate human fluoride exposure as closely as feasible. There were twelve rats in each group, four male rats and eight female rats. The male and female rats were caged and mated overnight according to a male to female ratio of 1:2. The females were separated and placed in separate cages once the vaginal plug was formed. Pregnant female rats were exposed to NaF from pregnancy until 21 days postdelivery. During the 21-day lactation phase, rat offspring were exposed to NaF through maternal breastfeeding. Next, twenty offspring (female: male = 1:1) were randomly selected from each group and provided with the same NaF-treatment as their

parents until PND 60 (Supplementary Fig. 1A). This dosage selection is based on the environmental fluoride levels in drinking water and previous research results (Wang et al., 2018; Zhang et al., 2020).

2.3. Cell culture and treatment

Human neuroblastoma SH-SY5Y cells were obtained from American Type Culture Collection (ATCC Inc., Manassas, VA, USA). The cells were grown in DMEM, supplemented with fetal bovine serum (10%, Biological Industries) at 37 ℃ under a humidified 5% CO_2 atmosphere. NaF was freshly supplied in distilled water to a stock solution of 4 g/L, and the selected dosages were 0, 20, 40, or 60 mg/L. The dosage was based on the calculated CCK-8 results, consistent with previous studies (Tu et al., 2018). The SH-SY5Y cells were seeded, and upon reaching 70–80% confluence, various concentrations of NaF for 24 h were added.

Additionally, to explore the roles of autophagosome-lysosome fusion in NaF-treated neurotoxicity, we utilized rapamycin at a stock concentration of 1 mmol/L. NaF (60 mg/L) with/without rapamycin (200 nmol/L, pre-treated for 1 h) was used to treat SH-SY5Y cells. Moreover, recombinant adenovirus with ATG14 overexpression (Ad-ATG14, MOI = 400) and control adenovirus (Vector) were developed. After being infected with Ad-ATG14 for 24 h, cells were treated with 60 mg/L NaF. Each cell culture experiment was repeated at least three times independently.

2.4. Morris water maze (MWM) test

The MWM task is extensively used to evaluate memory capacities and spatial learning, and we performed a slight modification according to previous literature (Qiao et al., 2005; Ji and Zhao, 2021). The MWM consists of a circular black painted pool (1.8 m in diameter and 0.5 m high), a platform (round, 8 cm in diameter), and a vidicon above the pool's center to capture the images of swimming rats connected to a tracking system. The pool was filled with water and mixed with nontoxic black ink (temperature was kept at 22 ± 2 ℃). The round platform was underwater and hidden in a fixed location (the target quadrant).

In the place navigation test (PNT), the training was carried out for 4 consecutive days, and 4 quadrants were measured every day with a different starting quadrant in each trial. The offspring faced the pool wall and entered the water from the midpoints of the four quadrants. The latency for each offspring rat to reach the platform was recorded. If the platform was found for 60 s, the rat was allowed to stand on the platform for 10 s; otherwise, the escape latency was recorded as 60 s, and the corresponding rat was placed on the platform for another 15 s. To assess the spatial learning ability of rats, the swimming distance, latency, and speed to the platform were measured. The spatial probe test (SPT) was carried out on the fifth day. The concealed platform was removed, and the rats were forced to swim for 60 s. The number of times that the rat passed through the previous platform site and the proportion of time and the swim distance spent searching for the platform were automatically recorded and used as a memory test.

2.5. Western blot

In the rat hippocampus and SH-SY5Y cells, RIPA lysis buffer was used to extract the total proteins. BCA assay kit was used to measure the total protein concentration in the samples. The protein samples were separated using SDS–PAGE and transferred onto polyvinylidene fluoride (PVDF) membranes. Using 5% skim milk blocked membranes for at least 1 h at room temperature, and incubated at 4 ℃ for 14–18 h with primary antibodies against p62 (1:1000), LC3 (1:500), caspase-3 (1:1000), PARP1 (1:1000), ATG14 (1:1000), STX17 (1:1000), SNAP29 (1:1000), VAMP8 (1:1000), β-actin (1:500), GAPDH (1:1000). Subsequently, after washing, the membranes were incubated for 2 h at room temperature with horseradish HRP-conjugated goat anti-rabbit IgG. After washing three times with TBST, the membrane signals were measured using ECL reagents (Advansta Inc., Menlo Park, CA, USA) and scanned with GeneGnome chemiluminescent imaging equipment (Syngene Inc., Frederick, MD, USA). The band intensities were measured using Image J (Rawak Software, Inc. Germany). Experiments were performed independently in triplicate.

2.6. Co-immunoprecipitation

Cells were lysed in IP lysis buffer. Eighty microliters of agarose A+G (50%) was added to each sample and incubated at 4 ℃ for 2 h. After removing protein A+G beads, 16 μg of Co-IP antibody ATG14 was added to 500 μL of total protein to react with the target protein and incubated overnight at 4 ℃. Then, 80 μL of 50% agarose protein A+G (30 μL/tube) was added to the sample and incubated at 4 ℃ for 6 h. Finally, boiling was used to elute immunoprecipitates, and samples were separated and blotted onto nitrocellulose membranes using conventional western blot techniques.

2.7. Statistical analysis

SPSS 26.0 software was used for statistical analysis. Multiple comparisons were performed by one-way ANOVA, followed by Tukey's multiple comparisons test. Water maze test data were analyzed using repeated measures analysis of variance. The results are shown as the mean ± standard deviation (SD), and a P value < 0.05 was considered statistically significant.

3. Results

3.1. Perinatal NaF exposure impairs memory and learning capacities in rats

The average escape latency for the PNT of the MWM test decreased in each group. The latency and swimming distance of the rats were significantly longer in the 100 mg/L NaF-treatment group than in the control group each day ($P < 0.05$). The swimming speed of the 50 and 100 mg/L NaF-treated rats were remarkably lower than those of control rats on the 1st day ($P < 0.05$) (Supplementary Fig. 1B–D). Furthermore, for the SPT of the MWM task, the results indicated that the number of platform crossing were notably diminished in the 50 and 100 mg/L NaF-treatment groups compared with the control group ($P < 0.05$). In addition, the rats in the 50 and 100 mg/L NaF groups spent immensely more time and distance further than the control group in the target quadrant where the platform was located ($P < 0.05$) (Supplementary Fig. 1E–G).

3.2. NaF exposure induces autophagic degradation and apoptosis in vitro and in vivo

As shown in Fig. 1A, B, the results revealed that compared with the control, the protein levels of LC3-II and p62 were remarkably enhanced in rats treated with 50 and 100 mg/L NaF ($P < 0.05$). Furthermore, as shown in Fig. 1C, D, in SH-SY5Y cells treated with 40 and 60 mg/L NaF, the protein expression levels of LC3-II and p62 were significantly higher than those in the control ($P < 0.05$). Subsequently, as shown in Fig. 1E, F, in comparison to the control group, rats treated with 25, 50, and 100 mg/L NaF had dramatically increased protein levels of cleaved-caspase-3. Consistent with these findings, the protein levels of cleaved-caspase-3

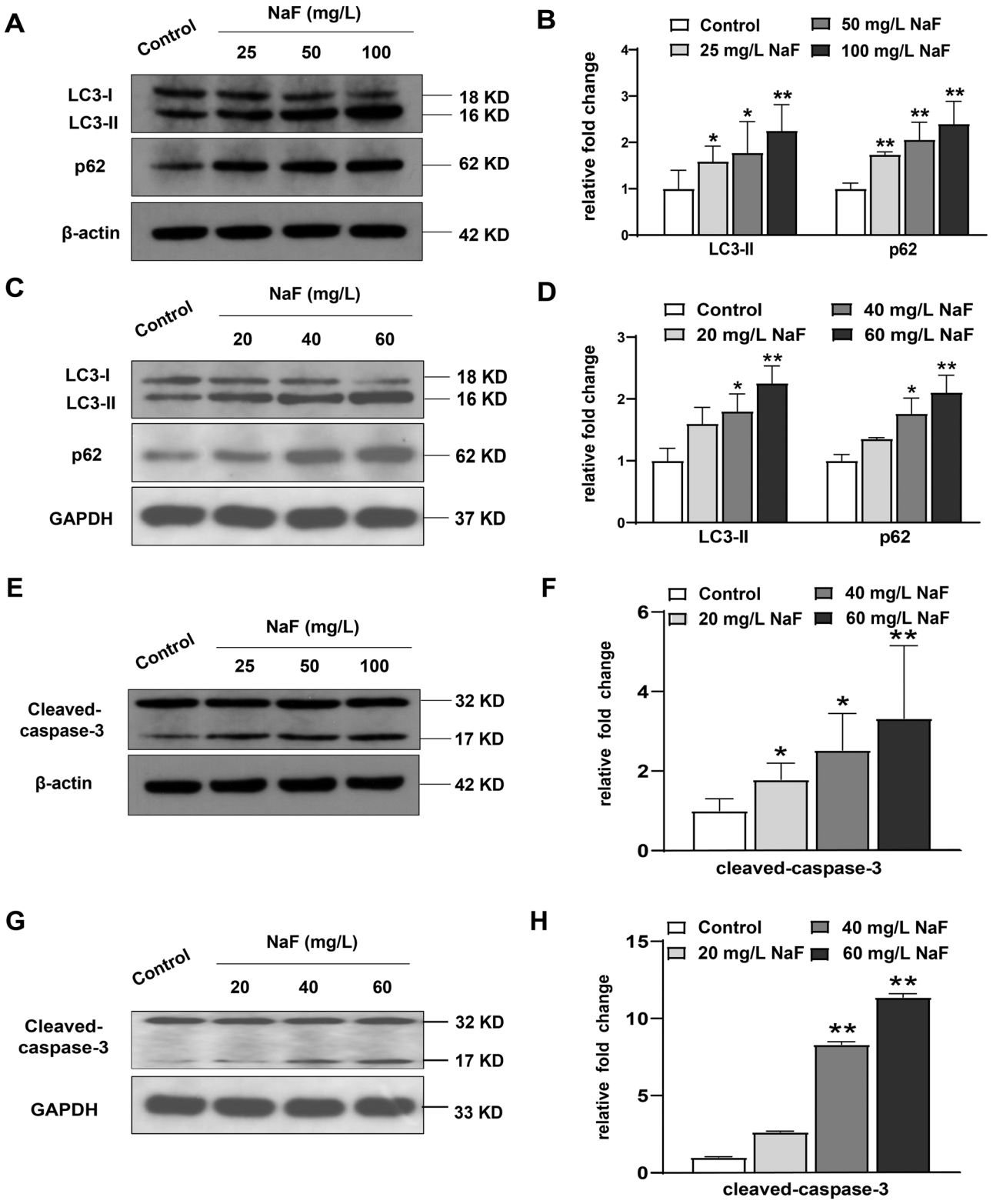

Fig. 1. NaF exposure induces autophagic degradation and apoptosis in vitro and in vivo. (A) Representative western blot images of the autophagy markers LC3-II and p62 in hippocampal tissues of adult rats. (B) Quantitative analyses of the autophagy markers LC3-II and p62 in hippocampal tissues of adult rats. (C) Representative western blot images of the autophagy markers LC3-II and p62 in SH-SY5Y cells. (D) Quantitative analyses of the autophagy markers LC3-II and p62 in SH-SY5Y cells. (E) Representative images of western blot for the apoptosis marker cleaved-caspase-3 in hippocampal tissues of adult rats. (F) Quantitative analyses of the apoptosis marker cleaved-caspase-3 in hippocampal tissues of adult rats. (G) Representative western blot of the apoptosis marker cleaved-caspase-3 in SH-SY5Y cells. (H) Quantitative analyses of the apoptosis marker cleaved-caspase-3 in SH-SY5Y cells. The data are presented as the means ± S.D. for three different experiments. $^{*}P < 0.05$ versus the control group. $^{**}P < 0.01$ versus the control group.

were significantly increased in NaF-treated SH-SY5Y cells ($P < 0.05$) (Fig. 1G, H). As indicated in Supplementary Fig. 2, compared with the control group, the cell viability dose-dependently declined starting from the 40 mg/L NaF treatment group ($P < 0.05$).

3.3. NaF exposure blocks autophagosome-lysosome fusion in vitro and in vivo

To determine whether NaF can affect autophagosome-lysosome fusion, we analyzed the state of autophagic flux by fluorescence. Since LC3 localizes to the autophagosome membrane and LAMP2 is a lysosomal marker protein, co-localization of LC3 and LAMP2 immunofluorescence was used to analyze autophagosome-lysosome fusion, where the yellow dots indicate the occurrence of autophagosome-lysosome fusion. As shown in Fig. 2A, the co-localization of LC3 and LAMP2 was significantly reduced after NaF treatment in NaF-treated rats. Supportively, the co-localization of LC3 and LysoTracker red was significantly reduced after NaF treatment in a dose-dependent manner in SH-SY5Y cells (Fig. 2B).

3.4. NaF exposure suppresses the formation of the SNARE complex in vitro and in vivo

As illustrated in Fig. 3A, B, the protein levels of STX17, SNAP29, and VAMP8 were markedly diminished in comparison to the control group in rats treated with 50 and 100 mg/L NaF ($P < 0.05$). Consistently, the protein levels of STX17, SNAP29, and VAMP8 were dramatically lower than those in the control group in SH-SY5Y cells ($P < 0.05$) (Fig. 3C, D).

3.5. NaF exposure inhibits the expression of ATG14 in vitro and in vivo

As shown in Fig. 4A, B, the ATG14 protein level in NaF-treated rats was remarkably lower than the control group ($P < 0.05$). In line with our in vivo findings, the protein level of ATG14 was dramatically lower than the control group in SH-SY5Y cells ($P < 0.05$) (Fig. 4C, D).

3.6. ATG14 overexpression promotes autophagy and reduces apoptosis induced by NaF treatment in SH-SY5Y cells

As illustrated in Fig. 5A, B, treatment with rapamycin decreased the protein level of p62 in the co-treatment group compared with the NaF group alone ($P < 0.05$); A similar trend was also observed when a combination treatment of Ad-ATG14 and NaF was used ($P < 0.05$). Additionally, the results showed that rapamycin and Ad-ATG14 both significantly decreased the protein level of cleaved-caspase-3 in the co-treatment group ($P < 0.05$) (Fig. 5B). Finally, compared with NaF treatment alone, the protein level of LC3-II was upregulated significantly after co-treatment using rapamycin and NaF ($P < 0.05$). Similarly, Ad-ATG14 also increased the expression level of LC3-II following NaF treatment ($P < 0.05$) (Fig. 5C, D).

3.7. ATG14 overexpression restores the interaction of ATG14 and the SNARE complex in NaF-treated SH-SY5Y cells

As shown in Fig. 6A, D, the results revealed that rapamycin and Ad-ATG14 significantly enhanced the protein levels of STX17, SNAP29, and VAMP8, in the co-treatment group ($P < 0.05$). Subsequently, compared with NaF treatment alone, the interaction between ATG14 and the SNARE complex increased after co-treatment with rapamycin and NaF. Ad-ATG14 also increased the interaction between ATG14 and the SNARE complex following NaF treatment (Fig. 6E).

4. Discussion

This study revealed that autophagosome-lysosome fusion blockage is a novel mechanism involved in NaF-induced developmental neurotoxicity. Notably, NaF impeded the formation of the SNARE complex by downregulating ATG14 to block autophagosome-lysosome fusion, resulting in fluoride-induced developmental neurotoxicity.

Many relevant studies collectively supported that fluoride has developmental neurotoxicity (Nadei et al., 2020; Farmus et al., 2021). Fluoride can enter the offspring's brain through the placental barrier and the blood-brain barrier during the perinatal period, which causes irreversible developmental damage to the nervous system (Li et al., 2013). Herein, to simulate the developmental neurotoxicity caused by fluoridated drinking water in humans, we developed a rat model of ingesting fluoridated water ad libitum from the pregnancy of parental rats until the offspring were two months old (covering the critical period of neurological development), and the offspring served as study subjects. The latency and swimming distance were both increased in NaF-treated rats, according to the PNT of the MWM test results. Furthermore, the SPT results demonstrated reduced platform crossing frequencies and decreased swimming time and distance in the target quadrant in the NaF-treatment group. Our results are akin to the study of Nadei et al. (2020), who revealed that excessive NaF exposure impaired spatial learning ability and long-term memory capacity in rats. Based on our findings, NaF treatment in rat offspring deteriorates the spatial learning ability and weakens memory retention capacity, suggesting that fluoride

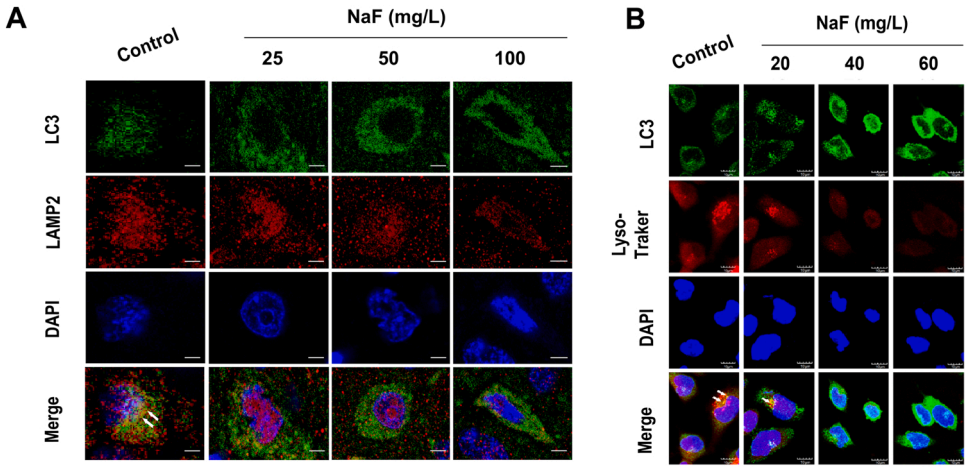

Fig. 2. NaF exposure blocks autophagosome-lysosome fusion in vitro and in vivo. (A) Representative images of immunofluorescence staining for LC3, LAMP2 and DAPI in the hippocampal CA3 region of adult rats. The scale bar represents 50 μm. (B) Representative images of immunofluorescence staining for LC3, LysoTracker red and DAPI in SH-SY5Y cells. The scale bar represents 50 μm.

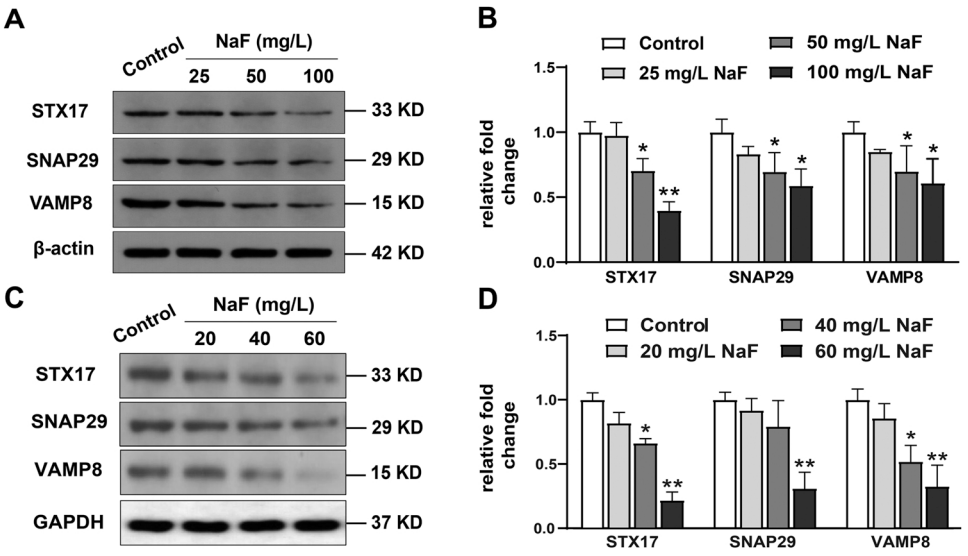

Fig. 3. NaF exposure suppresses the formation of the SNARE complex in vitro and in vivo. (A) Representative images of western blot for SNARE complex STX17, SNAP29 and VAMP8 in hippocampal tissues of adult rats. (B) Quantitative analyses of the SNARE complex STX17, SNAP29 and VAMP8 in hippocampal tissues of adult rats. (C) Representative images of western blot for SNARE complex STX17, SNAP29 and VAMP8 in SH-SY5Y cells. (D) Quantitative analyses of the SNARE complexes STX17, SNAP29 and VAMP8 in SH-SY5Y cells. The data are presented as the means ± S.D. for three different experiments. $^{*}P < 0.05$ versus the control group. $^{**}P < 0.01$ versus the control group.

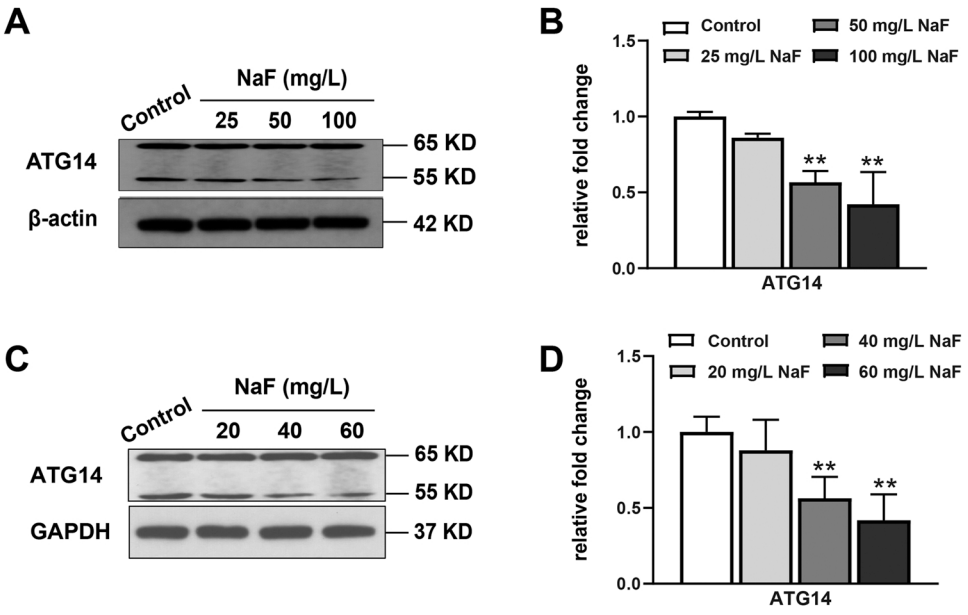

Fig. 4. NaF exposure inhibits the expression of ATG14 in vitro and in vivo. (A) Representative images of western blot for ATG14 in hippocampal tissues of adult rats. (B) Quantitative analyses of ATG14 in hippocampal tissues of adult rats. (C) Representative images of western blot for ATG14 in SH-SY5Y cells. (D) Quantitative analyses of ATG14 in SH-SY5Y cells. The data are presented as the means ± S.D. for three different experiments. $^{*}P < 0.05$ versus the control group. $^{**}P < 0.01$ versus the control group.

is a developmental neurotoxicant, which also demonstrated that the rat model for fluoride-induced developmental neurotoxicity was successfully developed.

Autophagic flux is a highly conserved catabolic process that degrades unnecessary substances in lysosomes for recycling (Galluzzi et al., 2017). Any dysfunction in the autophagic flux process can lead to defective autophagy and cell damage, which is the basis for several neurological diseases. In the present study, NaF increased the expression of LC3-II, which is located in the autophagosome membrane and whose expression is believed to be a reflection of the number of autophagosomes (Li et al., 2013). Therefore, increased expression of LC3-II in vivo and in vitro confirmed that NaF caused the accumulation of autophagosomes. Furthermore, our results showed that the expression of p62 improved in vivo and in vitro. Since p62 is a substrate preferentially degraded by autophagy, it interacts with LC3 to ensure that the substrate to be degraded is delivered to the autophagosome for degradation (Mizushima et al., 2010). Therefore, elevated expression of LC3-II and p62 usually indicates impaired autophagic degradation (González-Rodríguez et al., 2014). These results are in agreement with Niu et al. (2018) findings and confirm that NaF exposure restrains autophagic degradation, resulting in autophagic flux blockage.

Many studies have shown that autophagic flux blockage could cause cell apoptosis (Codogno and Morel, 2018). Our present results showed that excessive NaF exposure induced apoptosis in a dose-dependent manner, which was confirmed by the upregulated expression of cleaved-caspase-3 in vivo and in vitro. More recently, it has been shown that NaF exposure leads to defective autophagy, eliciting excessive apoptosis and inducing neurotoxicity (Mariño et al., 2014). In addition, our results are in line with a recent study showing that suppressing apoptosis could alleviate detrimental mitochondrial and cellular outcomes caused by NaF, thus promoting cell survival (Zhao et al., 2019). Nevertheless, promoting autophagy in neurons can either relieve or increase apoptosis, and the outcome following changed autophagy may differ in various neuronal cells. In SH-SY5Y cells, rapamycin alleviated the autophagic flux blockage and cell death induced by NaF (Zhou et al., 2019). In contrast, in PC12 cells, stimulation of autophagy by rapamycin aggravated PBDE-47-induced apoptosis and cell death (Li et al., 2019). Differences in varied interventions, cell-type specificity, dose sensitivity,

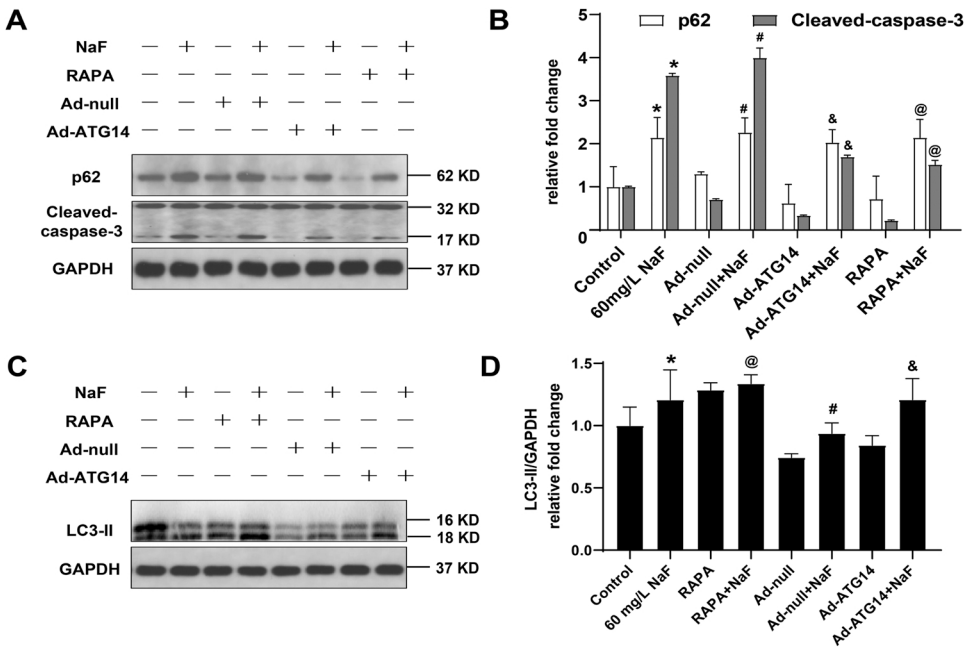

Fig. 5. ATG14 overexpression promotes autophagy and reduces apoptosis induced by NaF treatment in SH-SY5Y cells. (A) Representative images of western blot for p62 and cleaved-caspase-3 in SH-SY5Y cells after NaF combined with RAPA treatment and the combination of Ad-ATG14 infection and NaF treatment. (E) Quantitative analyses of p62 and cleaved-caspase-3 in SH-SY5Y cells. (F) Representative images of western blot for LC3-II in SH-SY5Y cells after NaF combined with RAPA treatment and combination of Ad-ATG14 infection and NaF treatment. (G) Quantitative analyses of LC3-II in SH-SY5Y cells. The data are presented as the means ± S.D. for three different experiments. $^{*}P < 0.05$ versus the control group. $^{\#}P < 0.05$ versus the Ad-null infection. $^{\&}P < 0.05$ versus the combination of Ad-null infection and NaF treatment group. $^{@}P < 0.05$ versus the NaF treatment group.

and duration of treatment may explain the inconsistencies. Overall, our results thus support the notion that NaF disrupts autophagic degradation, resulting in autophagic flux blockage and apoptosis in a dose-dependent manner.

Autophagosome-lysosome fusion is an indispensable step in maintaining robust autophagic flux, which is crucial for the cellular degradation and reuse of excess intracellular material by autophagic function (McLelland et al., 2016). The fusion of autophagosomes with lysosomes is controlled by a complex network of signaling pathways involving multiple steps and synergistic effects of numerous molecules, among which the SNARE complex is thought to play a pivotal role in the fusion process. In this study, our results showed that NaF treatment decreased the protein expression of STX17, SNAP29, and VAMP8 and blocked autophagosome-lysosome fusion. Knockout of any of these proteins prevents the formation of the STX17-SNAP29-VAMP8 complex, leading to autophagosome-lysosome fusion blockage (Tang et al., 2021). Previous studies identified STX17 as an autophagosomal SNARE that translocates to autophagosomes and interacts with SNAP29 and endo/lysosomal VAMP8 (Hamasaki et al., 2013). Moreover, our results coincide with reports in which EACC, a chemical modulator of autophagy, inhibited the translocation of autophagosome-specific STX17 and caused a massive accumulation of LC3-II, thereby blocking autophagosome-lysosome fusion (Vats and Manjithaya, 2019). Thus, our findings suggested that fluoride may disrupt the formation of the SNARE complex by impairing STX17 loading onto autophagosomes. Interestingly, O-GlcNAcylation of SNAP29 has been shown to prevent the interaction of STX17 with VAMP8, preventing autophagosome-lysosome fusion and proper flux through the autophagy pathway. Supportively, As (III) can block SNARE complex formation by enhancing O-GlcNAcylation of SNAP29 (Dodson et al., 2018). Berbamine (BBM), a natural substance derived from traditional Chinese medicine, has been shown to impede autophagosome-lysosome fusion by interfering with the interaction of SNAP29 and VAMP8 (Fu et al., 2018). Altogether, we provide persuasive evidence that NaF blocks autophagosome-lysosome fusion and suppresses the formation of the STX17-SNAP29-VAMP8 complex, thereby participating in the occurrence and development of fluoride neurotoxicity.

Multiple factors precisely regulate autophagosome-lysosome fusion, and ATG14 is a decisive switch that regulates autophagic SNARE-mediated membrane fusion temporally and spatially (Itakura and Mizushima, 2013). Herein, our results showed that NaF treatment inhibits ATG14 expression in vivo and in vitro, implying that NaF may inhibit autophagosome-lysosome fusion by downregulating ATG14 expression. To reveal the role of ATG14-mediated autophagosome-lysosome fusion dysfunction in fluoride-induced neurotoxicity, we developed a genetic autophagy stimulation model by upregulation of ATG14 to modulate autophagy. Our results showed that upregulation of ATG14 elevates the protein level and formation of the STX17-SNAP29-VAMP8 complex, and enhanced the interaction of ATG14 and the STX17-SNAP29-VAMP8 complex. Furthermore, upregulation of ATG14 also promoted autophagosome-lysosome fusion. Mechanistically, in the present study, ATG14 might form a clasp to bind to the autophagosome binary and prime it for binding to VAMP8 on lysosomes. The ATG14 coiled-coil domain (CCD) interacts with the helix of the STX17 SNARE motif, and this interaction is essential for its fusion-promoting activity, which allows ATG14 to function as a clasp to stabilize the helical structure formed by STX17 and SNAP29 (Liu et al., 2015). Together, upregulation of ATG14 can promote autophagosome-lysosome fusion by enhancing the interaction of ATG14 and the STX17-SNAP29-VAMP8 complex. Consistently, Zhang et al. (2021) found that upregulation of ATG14 in macrophages improved autophagosome-lysosome fusion, and corrected autophagy dysfunction in apoe-/- mice plaque macrophages. Moreover, FoxO1 mediated AGE-induced EC autophagic apoptosis by impairing autophagosome-lysosome fusion by inhibiting ATG14 expression (Zhang et al., 2019b). Altogether, our results further revealed a crucial role of ATG14 upregulation in promoting autophagosome-lysosome fusion by improving the stability of the STX17-SNAP29-VAMP8 complex.

Interestingly, our findings demonstrated that upregulation of ATG14 not only promotes autophagosome-lysosome fusion but also alleviates NaF-induced autophagic flux blockage, which reduces cell apoptosis. Although the nervous system is a preferential target for uncovering autophagy abnormalities, the functional roles of autophagy in neuronal physiology or in pathological aspects of neuronal disorders are still limited, and growing evidence has revealed that the protein levels of the autophagy marker p62 accumulate in neurons of various neurological disorders, including Alzheimer's diseases, Parkinson disease, cadmium or lead-induced neurotoxicity (Zhang et al., 2019a; Cai and Ganesan, 2021; Li et al., 2022). Similarly, we found that upregulation of ATG14

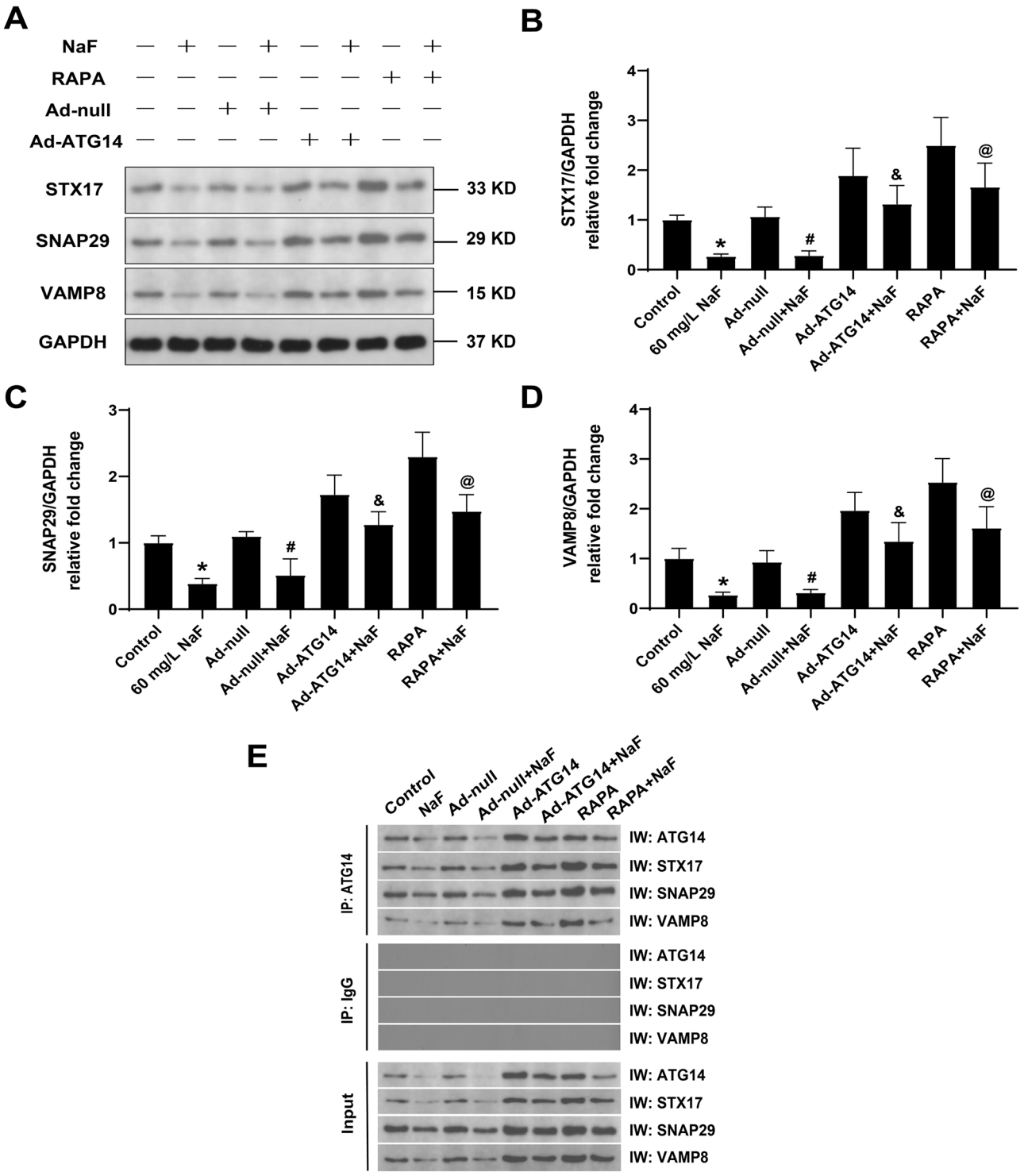

Fig. 6. ATG14 overexpression restores the interaction of ATG14 and the SNARE complex in NaF-treated SH-SY5Y cells. (A) Representative images of western blot for SNARE complex STX17, SNAP29 and VAMP8 in SH-SY5Y cells after NaF combined with RAPA treatment and combination of Ad-ATG14 infection and NaF treatment. (B) Quantitative analyses of STX17 in SH-SY5Y cells. (C) Quantitative analyses of SNAP29 in SH-SY5Y cells. (D) Quantitative analyses of VAMP8 in SH-SY5Y cells. (E) Co-precipitation of the SNARE complex with ATG14 after NaF combined with RAPA treatment and the combination of Ad-ATG14 infection and NaF treatment. The data are presented as the means ± S.D. for three different experiments. $^{*}P < 0.05$ versus the control group. $^{\#}P < 0.05$ versus the Ad-null infection. $^{\&}P < 0.05$ versus the combination of Ad-null infection and NaF treatment group. $^{@}P < 0.05$ versus the NaF treatment group.

reduces p62 expression in SH-SY5Y cells after NaF treatment, consistent with other studies (Zhang et al., 2021). Moreover, reducing p62 is a consequence of restoring autophagic flux, and it is well documented that autophagy or autophagic degradation acts as a protective mechanism required for cell health and survival, while its defects have been implicated in cell loss (Green and Levine, 2014). Thus, autophagic flux blockage likely contributes to neuronal death, and robust autophagic flux can facilitate cell survival, supported by the decreased marker of apoptosis after upregulating ATG14. Similar results showed that siRNA-mediated genetic inhibition of ATG14 enhanced

cisplatin-mediated cell growth inhibition and cell death in cisplatin-resistant cells (He et al., 2015). Nevertheless, contrary to the present work, another study showed that the overexpression of ATG14 in HeLa cells inhibited cell viability and increased mitochondrial apoptosis and endoplasmic reticulum stress (ER stress) (Mukhopadhyay et al., 2017); ER stress induced by ATG14 was due to FFA accumulation-mediated ROS induction, which resulted in the collapse of mitochondrial membrane potential, decreasing ATP levels, which acts as a powerful stimulus of cellular death. In addition, differences in the types of cell lines, dose sensitivity, and treatment duration also seem to be responsible for the different apoptosis outcomes. It should be noted that our results are consistent with a previous study that reported that overexpression of ATG14 inhibited apoptosis and secretion of the inflammatory cytokines IL-2, IL-6, and INFG in Ox-LDL-treated macrophages, alleviating the damage to cells (Zhang et al., 2021). Hence, our results revealed a vital role for ATG14 upregulation in providing protection by restoring autophagic flux, which removes misfolded proteins and damaged organelles, thus reducing cell apoptosis and death.

5. Conclusion

In conclusion, our in vivo and in vitro data provide evidence that NaF exposure leads to autophagosome-lysosome fusion dysfunction by blocking the formation of the SNARE complex, resulting in autophagic flux blockage and apoptosis. In particular, our findings also revealed that upregulation of ATG14 effectively regulates SNARE complex formation, thereby promoting autophagosome-lysosome fusion and alleviating developmental fluoride-induced neurotoxicity. These findings provide new insights into the mechanisms of fluoride neurotoxicity and offer a promising therapeutic target to reduce fluoride-induced developmental neurotoxicity. Further study is needed to elucidate the detailed molecular mechanism by which ATG14 promotes SNARE complex formation, thus providing a scientific basis for preventing and controlling developmental neurotoxicity resulting from fluoride exposure.

Funding

This work was supported by grants from the National Natural Science Foundation of China (Grant Nos. 81860559 and 82060580), the Program of Science and Technology Innovation in Bingtuan (Grant No. 2021CB046), and the High-Level Talent Research Project of Shihezi University (Grant No. RCZK2018C02).

CRediT authorship contribution statement

Yuanli Zhang: Methodology, Formal analysis, Writing – original draft. **Xie Han:** Methodology, Writing – review & editing. **Yanling Tang:** Writing – review & editing. **Jingjing Zhang:** Visualization, Investigation. **Zeyu Hu:** Visualization, Investigation. **Wanjing Xu:** Investigation. **Ping Yao:** Writing – review & editing. **Qiang Niu:** Conceptualization, Resources, Writing – review & editing, Funding acquisition.

Declaration of Competing Interest

The authors declare that they have no known competing financial interests or personal relationships that could have appeared to influence the work reported in this paper.

Appendix A. Supplementary material

Supplementary data associated with this article can be found in the online version at doi:10.1016/j.ecoenv.2021.113108.

References

Bartos, M., Gumilar, F., Gallegos, C.E., Bras, C., Dominguez, S., Mónaco, N., Esandi, M.D. C., Bouzat, C., Cancela, L.M., Minetti, A., 2018. Alterations in the memory of rat offspring exposed to low levels of fluoride during gestation and lactation: involvement of the α7 nicotinic receptor and oxidative stress. Reprod. Toxicol. 81, 108–114.

Bernard, A., Klionsky, D.J., 2015. Toward an understanding of autophagosome-lysosome fusion: the unsuspected role of ATG14. Autophagy 11 (4), 583–584.

Caglayan, C., Kandemir, F.M., Darendelioğlu, E., Küçükler, S., Ayna, A., 2021. Hesperidin protects liver and kidney against sodium fluoride-induced toxicity through anti-apoptotic and anti-autophagic mechanisms. Life Sci. 281, 119730.

Cai, Q., Ganesan, D., 2021. Regulation of neuronal autophagy and the implications in neurodegenerative diseases. Neurobiol. Dis., 105582

Codogno, P., Morel, E., 2018. FOXO3a provides a quickstep from autophagy inhibition to apoptosis in cancer therapy. Dev. Cell 44 (5), 537–539.

Cui, Y., Zhang, B., Ma, J., Wang, Y., Zhao, L., Hou, C., Yu, J., Zhao, Y., Zhang, Z., Nie, J., Gao, T., Zhou, G., Liu, H., 2018. Dopamine receptor D2 gene polymorphism, urine fluoride, and intelligence impairment of children in China: a school-based cross-sectional study. Ecotoxicol. Environ. Saf. 165, 270–277.

Diao, J., Liu, R., Rong, Y., Zhao, M., Zhang, J., Lai, Y., Zhou, Q., Wilz, L.M., Li, J., Vivona, S., Pfuetzner, R.A., Brunger, A.T., Zhong, Q., 2015. ATG14 promotes membrane tethering and fusion of autophagosomes to endolysosomes. Nature 520 (7548), 563–566.

Dodson, M., Liu, P., Jiang, T., Ambrose, A., Luo, G., Rojo de la Vega, M., Cholanians, A., Wong, P., Chapman, E., Zhang, D.J., 2018. Increased O-GlcNAcylation of SNAP29 drives arsenic-induced autophagic dysfunction. Mol. Cell Biol. 38 (11) e00595-17.

Farmus, L., Till, C., Green, R., Hornung, R., Martinez Mier, E.A., Ayotte, P., Muckle, G., Lanphear, B.P., Flora, D.B., 2021. Critical windows of fluoride neurotoxicity in Canadian children. Environ. Res. 200, 111315.

Fu, R., Deng, Q., Zhang, H., Hu, X., Li, Y., Liu, Y., Hu, J., Luo, Q., Zhang, Y., Jiang, X., Li, L., Yang, C., Gao, N., 2018. A novel autophagy inhibitor berbamine blocks SNARE-mediated autophagosome-lysosome fusion through upregulation of BNIP3. Cell Death Dis. 9 (2), 243.

Galluzzi, L., Baehrecke, E.H., Ballabio, A., Boya, P., Bravo-San Pedro, J.M., Cecconi, F., Choi, A.M., Chu, C.T., Codogno, P., Colombo, M.I., Cuervo, A.M., Debnath, J., Deretic, V., Dikic, I., Eskelinen, E.L., Fimia, G.M., Fulda, S., Gewirtz, D.A., Green, D. R., Hansen, M., Harper, J.W., Jäättelä, M., Johansen, T., Juhasz, G., Kimmelman, A. C., Kraft, C., Ktistakis, N.T., Kumar, S., Levine, B., Lopez-Otin, C., Madeo, F., Martens, S., Martinez, J., Melendez, A., Mizushima, N., Münz, C., Murphy, L.O., Penninger, J.M., Piacentini, M., Reggiori, F., Rubinsztein, D.C., Ryan, K.M., Santambrogio, L., Scorrano, L., Simon, A.K., Simon, H.U., Simonsen, A., Tavernarakis, N., Tooze, S.A., Yoshimori, T., Yuan, J., Yue, Z., Zhong, Q., Kroemer, G., 2017. Molecular definitions of autophagy and related processes. EMBO J. 1811–1836.

González-Rodríguez, A., Mayoral, R., Agra, N., Valdecantos, M., Pardo, V., Miquilena-Colina, M., Vargas-Castrillón, J., Lo Iacono, O., Corazzari, M., Fimia, G., Piacentini, M., Muntané, J., Boscá, L., García-Monzón, C., Martín-Sanz, P., Valverde, Á.J., 2014. Impaired autophagic flux is associated with increased endoplasmic reticulum stress during the development of NAFLD. Cell Death Dis. 5 (4), e1179.

Green, D.R., Levine, B., 2014. To be or not to be? How selective autophagy and cell death govern cell fate. Cell 157 (1), 65–75.

Green, R., Lanphear, B., Hornung, R., Flora, D., Martinez-Mier, E.A., Neufeld, R., Ayotte, P., Muckle, G., Till, C., 2019. Association between maternal fluoride exposure during pregnancy and IQ scores in offspring in Canada. JAMA Pediatr. 173 (10), 940–948.

Hamasaki, M., Furuta, N., Matsuda, A., Nezu, A., Yamamoto, A., Fujita, N., Oomori, H., Noda, T., Haraguchi, T., Hiraoka, Y., Amano, A., Yoshimori, T., 2013. Autophagosomes form at ER-mitochondria contact sites. Nature 495 (7441), 389–393.

He, J., Yu, J.J., Xu, Q., Wang, L., Zheng, J.Z., Liu, L.Z., Jiang, B.H., 2015. Downregulation of ATG14 by EGR1-MIR152 sensitizes ovarian cancer cells to cisplatin-induced apoptosis by inhibiting cyto-protective autophagy. Autophagy 11 (2), 373–384.

Hu, Y.H., Wu, S.S., 1988. Fluoride in cerebrospinal fluid of patients with fluorosis. J. Neurol. Neurosurg. Psychiatry 51 (12), 1591–1593.

Itakura, E., Mizushima, N., 2013. Syntaxin 17: the autophagosomal SNARE. Autophagy 9 (6), 917–919.

Ji, C., Zhao, H., Chen, D., Zhang, H., Zhao, Y.J., 2021. β-propeller proteins WDR45 and WDR45B regulate autophagosome maturation into autolysosomes in neural cells. Curr. Biol. 31 (8), 1666–1677.e6.

Ji, C., Zhao, Y.J.A., 2021. The BPAN and intellectual disability disease proteins WDR45 and WDR45B modulate autophagosome-lysosome fusion. Autophagy 17 (7), 1783–1784.

Khattak, J.A., Farooqi, A., Hussain, I., Kumar, A., Singh, C.K., Mailloux, B.J., Bostick, B., Ellis, T., van Geen, A., 2022. Groundwater fluoride across the Punjab plains of Pakistan and India: distribution and underlying mechanisms. Sci. Total Environ. 806 (Pt. 3), 151353.

Li, H., Zheng, T., Lian, F., Xu, T., Yin, W., Jiang, Y., 2022. Anthocyanin-rich blueberry extracts and anthocyanin metabolite protocatechuic acid promote autophagy-lysosomal pathway and alleviate neurons damage in in vivo and in vitro models of Alzheimer's disease. Nutrition 93, 111473.

Li, P., Ma, R., Dong, L., Liu, L., Zhou, G., Tian, Z., Zhao, Q., Xia, T., Zhang, S., Wang, A., 2019. Autophagy impairment contributes to PBDE-47-induced developmental neurotoxicity and its relationship with apoptosis. Theranostics 9 (15), 4375–4390.

Li, W., Tang, Y., Fan, Z., Meng, Y., Yang, G., Luo, J., Ke, Z.J., 2013. Autophagy is involved in oligodendroglial precursor-mediated clearance of amyloid peptide. Mol. Neurodegener. 8, 27.
Liu, R., Zhi, X., Zhong, Q., 2015. ATG14 controls SNARE-mediated autophagosome fusion with a lysosome. Autophagy 11 (5), 847–849.
Mariño, G., Niso-Santano, M., Baehrecke, E.H., Kroemer, G., 2014. Self-consumption: the interplay of autophagy and apoptosis. Nat. Rev. Mol. Cell Biol. 15 (2), 81–94.
Martínez, M., Lopez-Torres, B., Rodríguez, J., Martínez, M., Maximiliano, J., Martínez-Larrañaga, M., Anadón, A., Ares, I.J.F., 2020. Toxicologic evidence of developmental neurotoxicity of Type II pyrethroids cyfluthrin and alpha-cypermethrin in SH-SY5Y cells. Food Chem. Toxicol. 137, 111173.
McLelland, G.L., Lee, S.A., McBride, H.M., Fon, E.A., 2016. Syntaxin-17 delivers PINK1/parkin-dependent mitochondrial vesicles to the endolysosomal system. J. Cell Biol. 214 (3), 275–291.
Melila, M., Rajaram, R., Ganeshkumar, A., Kpemissi, M., Pakoussi, T., Agbere, S., Lazar, I. M., Lazar, G., Amouzou, K., Paray, B.A., Gulnaz, A., 2022. Assessment of renal and hepatic dysfunction by co-exposure to toxic metals (Cd, Pb) and fluoride in people living nearby an industrial zone. J. Trace Elem. Med. Biol. 69, 126890.
Mizushima, N., Yoshimori, T., Levine, B.J.C., 2010. Methods in mammalian autophagy research. Cell 140 (3), 313–326.
Mukhopadhyay, S., Schlaepfer, I.R., Bergman, B.C., Panda, P.K., Praharaj, P.P., Naik, P. P., Agarwal, R., Bhutia, S.K., 2017. ATG14 facilitated lipophagy in cancer cells induce ER stress mediated mitoptosis through a ROS dependent pathway. Free Radic. Biol. Med. 104, 199–213.
Nadei, O.V., Khvorova, I.A., Agalakova, N.I., 2020. Cognitive decline of rats with chronic fluorosis is associated with alterations in hippocampal calpain signaling. Biol. Trace Elem. Res. 197 (2), 495–506.
Niu, Q., Chen, J., Xia, T., Li, P., Zhou, G., Xu, C., Zhao, Q., Dong, L., Zhang, S., Wang, A., 2018. Excessive ER stress and the resulting autophagic flux dysfunction contribute to fluoride-induced neurotoxicity. Environ. Pollut. 233, 889–899.
O'Mullane, D.M., Baez, R.J., Jones, S., Lennon, M.A., Petersen, P.E., Rugg-Gunn, A.J., Whelton, H., Whitford, G.M., 2016. Fluoride and oral health. Community Dent. Health 33 (2), 69–99.
Qiao, D., Seidler, F., Slotkin, T.J.T., 2005. Oxidative mechanisms contributing to the developmental neurotoxicity of nicotine and chlorpyrifos. Toxicol. Appl. Pharmacol. 206 (1), 17–26.
Tang, Q., Gao, P., Arzberger, T., Höllerhage, M., Herms, J., Höglinger, G., Koeglsperger, T., 2021. Alpha-synuclein defects autophagy by impairing SNAP29-mediated autophagosome-lysosome fusion. Cell Death Dis. 12 (10), 854.
Tu, W., Zhang, Q., Liu, Y., Han, L., Wang, Q., Chen, P., Zhang, S., Wang, A., Zhou, X., 2018. Fluoride induces apoptosis via inhibiting SIRT1 activity to activate mitochondrial p53 pathway in human neuroblastoma SH-SY5Y cells. Toxicol. Appl. Pharmacol. 347, 60–69.
Vats, S., Manjithaya, R., 2019. A reversible autophagy inhibitor blocks autophagosome-lysosome fusion by preventing Stx17 loading onto autophagosomes. Mol. Biol. Cell 30 (17), 2283–2295.
Wang, J., Zhang, Y., Guo, Z., Li, R., Xue, X., Sun, Z., Niu, R., 2018. Effects of perinatal fluoride exposure on the expressions of miR-124 and miR-132 in hippocampus of mouse pups. Chemosphere 197, 117–122.
Wong, E., Cuervo, A.J., 2010. Autophagy gone awry in neurodegenerative diseases. Nat. Neurosci. 13 (7), 805–811.
Zhang, C., Huo, S., Fan, Y., Gao, Y., Yang, Y., Sun, D., 2020. Autophagy may be involved in fluoride-induced learning impairment in rats. Biol. Trace Elem. Res. 193 (2), 502–507.
Zhang, H., Dong, X., Zhao, R., Zhang, R., Xu, C., Wang, X., Liu, C., Hu, X., Huang, S., Chen, L., 2019a. Cadmium results in accumulation of autophagosomes-dependent apoptosis through activating Akt-impaired autophagic flux in neuronal cells. Cell Signal. 55, 26–39.
Zhang, H., Ge, S., He, K., Zhao, X., Wu, Y., Shao, Y., Wu, X., 2019b. FoxO1 inhibits autophagosome-lysosome fusion leading to endothelial autophagic-apoptosis in diabetes. Cardiovasc. Res. 115 (14), 2008–2020.
Zhang, H., Ge, S., Ni, B., He, K., Zhu, P., Wu, X., Shao, Y., 2021. Augmenting ATG14 alleviates atherosclerosis and inhibits inflammation via promotion of autophagosome-lysosome fusion in macrophages. Autophagy 1–13.
Zhao, Q., Niu, Q., Chen, J., Xia, T., Zhou, G., Li, P., Dong, L., Xu, C., Tian, Z., Luo, C., Liu, L., Zhang, S., Wang, A., 2019. Roles of mitochondrial fission inhibition in developmental fluoride neurotoxicity: mechanisms of action in vitro and associations with cognition in rats and children. Arch. Toxicol. 93 (3), 709–726.
Zhou, G., Tang, S., Yang, L., Niu, Q., Chen, J., Xia, T., Wang, S., Wang, M., Zhao, Q., Liu, L., Li, P., Dong, L., Yang, K., Zhang, S., Wang, A., 2019. Effects of long-term fluoride exposure on cognitive ability and the underlying mechanisms: role of autophagy and its association with apoptosis. Toxicol. Appl. Pharmacol. 378, 114608.